

Submitted: 08/08/2023

Accepted: 15/12/2023

Published: 31/12/2023

## Immunohistochemical and histochemical analysis of the rat skin after local electron irradiation

Grigory Demyashkin<sup>1,2\*</sup> , Yelena Shapovalova<sup>3</sup> , Anna Marukyan<sup>3</sup> , Matvey Vadyukhin<sup>1</sup> , Liia Alieva<sup>1</sup> , Nargiz Guseynova<sup>1</sup> , Sergey Koryakin<sup>2</sup> , Marina Filimonova<sup>2</sup> , Petr Shegay<sup>2</sup>  and Andrei Kaprin<sup>2</sup> 

<sup>1</sup>Sechenov University, Moscow, Russia

<sup>2</sup>National Medical Research Radiological Centre of the Ministry of Health of the Russian Federation, Moscow, Russia

<sup>3</sup>V.I. Vernadsky Crimean Federal University, Simferopol, Russia

### Abstract

**Background:** Skin cancer is the most frequently diagnosed type of cancer among all malignant neoplasms. The decrease in mitotic activity and the death of intact keratinocytes arise due to the constantly renewing epithelium being highly sensitive to ionizing radiation.

**Aim:** The aim of the study is immunohistochemical evaluation of the proliferative-apoptotic balance of keratinocytes, the fibrous component of the skin, and the expression of pro-inflammatory and anti-inflammatory cytokines after single or fractional local electron irradiation.

**Methods:** Wistar rats ( $n = 80$ ) were taken from the ITM&B Vivarium (Sechenov University) and divided into groups: I—control, which were injected with saline; and experimental groups, local electron irradiation at doses: II—8 Gy (single), III—40 Gy (single), IV—summary dose 78 Gy (fractional; 13 Gy per day for 6 days). We performed histological analysis, histochemical analysis using Masson, safranin, and picosirius red staining, immunohistochemical (Ki-67, caspase-3, p53, types I and III collagens, IL-1, IL-6, IL-4, and IL-10) and morphometric analysis of skin fragments of the outer surface of the thigh, irradiated in accordance with the design of the experiment. The early and delayed effects of local electron irradiation at different doses were studied.

**Results:** After local electron irradiation, dose-dependent morphological changes in the skin of the experimental groups were observed: violation of the histoarchitectonics of the skin confirmed by morphological and morphometric analysis, the proliferation of connective tissue according to the results of histochemical and immunohistochemical studies with signs of the radiation-induced skin fibrosis development, an increase in the levels of pro- and anti-inflammatory cytokines. We observed the most pronounced signs of radiation-induced skin damage in the group of fractional irradiation after 3 months.

**Conclusion:** 8 Gy and 40 Gy single local electron irradiation leads to a shift in the proliferative-apoptotic balance of keratinocytes toward their apoptosis, which activity is directly correlated with the dose of ionizing radiation, and 78 Gy in fractions leads to partial desquamation of the epithelium and inflammatory infiltration. In addition, after 3 months a significant increase in the expression of type I and III collagen fibers and the development of radiation-induced skin fibrosis takes place against the background of 78 Gy fractional local electron irradiation.

**Keywords:** Electron irradiation, Immunohistochemistry, Keratinocytes, Radiation-induced skin fibrosis.

### Introduction

Skin cancer is the most frequently diagnosed type of cancer among all malignant neoplasms (Perez *et al.*, 2022). Nonmelanoma skin cancer is divided into basal cell carcinoma and squamous cell carcinoma through the development and spread of the oncological process, prognosis, and morphological features (Cives *et al.*, 2020). Radiation therapy for nonmelanoma skin cancer is used by oncodermatologists and radiobiologists in ineffective surgical treatment as well as adjuvant or

palliative therapy (Pashazadeh *et al.*, 2019). In this case, brachytherapy, hypofractionated, and traditionally fractionated contact or surface irradiation with photons or X-rays are used, and the dose is selected individually, on average, for young people fractions in doses of 2–2.5 Gy, and for the elderly in doses of 3–5 Gy and more (Chua *et al.*, 2019). The damage to paratumoral tissues is often noted in the form of desquamation of the epithelium, necrosis of soft tissues, cartilage, and bone; pigmentary changes, telangiectasias, fibrosis,

\*Corresponding Author: Grigory A. Demyashkin. Sechenov University, Moscow, Russia.

Email: [dr.dga@mail.ru](mailto:dr.dga@mail.ru)

Articles published in Open Veterinary Journal are licensed under a Creative Commons Attribution-NonCommercial 4.0 International License



and skin atrophy, despite the relatively light doses and fractionation modes (Olschewski *et al.*, 2006).

The fewest side effects are described in single works after fractional electron irradiation in total doses of 44 Gy and 54 Gy (van Hezewijk *et al.*, 2010). However, the mechanisms of post-radiation damage have not been fully elucidated, and studies of the cell cycle of keratinocytes are few and remain elusive. The cell cycle of keratinocytes is regulated by proliferation proteins (Ki-67) and caspases, which are responsible for apoptosis. The high mitotic activity of keratinocytes of the constantly renewed skin epithelium makes them highly sensitive to radiation exposure (Borrelli *et al.*, 2019).

The fibrosis of the skin structures is the most common complication of radiotherapy. An imbalance in the synthesis and metabolism of different types of collagen fibers plays an important role in the formation of fibrosis and is regulated by pro-inflammatory cytokines such as IL-1 and IL-6 and anti-inflammatory cytokines such as IL-4 and IL-10 (Müller and Meineke, 2007). Type I collagen fibers give stability to the dermis, and type III collagen fibers provide elasticity and tensile strength. Degradation of type I and III collagen fibers is initiated by matrix metalloproteinases-1 (MMP-1) and MMP-3, respectively (Zhang *et al.*, 2014). An increase in the synthesis of RNA of type I and III collagen fibers in the superficial layers of the dermis after high-dose irradiation for breast cancer was found using the *in situ* hybridization. An increase in the level of aminoterminal type I collagen propeptides-positive fibroblasts in irradiated skin is shown by an immunohistochemical study. The authors have concluded that irradiation increases the expression of skin collagen genes, which are responsible for the development of fibrosis and thickening of the dermis. On the contrary, the same authors noted a change in the structure of collagen fibers to amorphous in recent studies using X-irradiation at a dose of 15 Gy. Temporary damage to the sebaceous glands and hair follicles without signs of inflammation, cell proliferation, or fibrosis was found. It differs from previously described results in the skin from other parts of the body (Borrelli *et al.*, 2019; da Silva Santin *et al.*,

2020). Therefore, the problem of radiation-induced fibrosis (RIF) is still relevant.

Thus, the creation of experimental models for studying the proliferative-apoptotic balance of keratinocytes and the fibrous component of the skin will make it possible to assess the degree and depth of skin post-radiation damage. In addition, such studies can help in choosing optimal radiotherapy doses and improve methods for the prevention of RIF.

#### Objectives of the study

Immunohistochemical evaluation of the proliferative-apoptotic balance of keratinocytes, the fibrous component of the skin, and the expression of pro-inflammatory and anti-inflammatory cytokines after single or fractional local electron irradiation and assessment of acute and delayed effects.

### Materials and Methods

#### Experimental design

Wistar rats ( $n = 80$ ; weight  $220 \pm 20$  g; age 9–10 weeks) were taken and divided into four groups. The day the experiment started was seen as the last day of local electron irradiation (Table 1).

#### Ionizing radiation

Animals were exposed to local irradiation of the skin of the outer surface thigh (dose rate 1 Gy/minute, energy 10 MeV and frequency 9 Hz, field size  $\varnothing$  100 mm) using a linear accelerator (“NOVAC-11”, National Medical Research Radiological Centre, Obninsk, Russia). The most commonly used doses in preclinical studies were chosen, equivalent to those used in clinical practice in the treatment of nonmelanoma malignant skin tumors (with single irradiation—8 Gy and 40 Gy, with a fractional regimen—a total dose of 78 Gy in fractions of 13 Gy), taking into account not only basal cell carcinoma and squamous cell carcinoma but also skin lymphoma, as well as percutaneous radiation exposure in case of malignant neoplasms of other localizations, which fits into a wide range of doses for their treatment. Animals were sedated before irradiation by a single injection of ketamine (50 mg/kg, intramuscularly) and xylazine (5 mg/kg, intraperitoneally). Then, they were moved to the object table and laid in such a way that the

Table 1. Experimental design.

Group	n	Effect	Manipulations
I—control	10	Acute (day 10)	Saline injections
	10	Delayed (day 90)	
II—experimental	10	Acute (day 10)	Single local electron irradiation, dose—8 Gy
	10	Delayed (day 90)	
III—experimental	10	Acute (day 10)	Single local electron irradiation, dose—40 Gy
	10	Delayed (day 90)	
IV—experimental	10	Acute (day 10)	Fractional local electron irradiation, dose—78 Gy (13 Gy daily for 6 days)
	10	Delayed (day 90)	

outer surface of the thigh was in the irradiation zone, while the lungs and heart remained outside this zone. Animals were removed from the experiment by ketamine+xylazine high concentrations in accordance with the design of the experiment.

The Radiation Therapy Oncology Group (RTOG) acute radiation morbidity scoring criteria and RTOG/European Organisation for Research and Treatment of Cancer (EORTC) late radiation morbidity scoring scheme were used to assess early (acute) and delayed side effects of radiotherapy.

**Histological examination**

Skin fragments after fixation in a buffered formalin solution were prepared according to a standard protocol and stained with hematoxylin and eosin. The obtained histological micropreparations were analyzed by three blinded pathologists in 10 fields of view of a light microscope.

**Histochemical examination**

One slide from each batch was stained with Masson, safranin, and picosirius red. For the specific detection of collagen fibers and assessment of the degree of fibrosis in the dermis, the histochemical staining method according to Masson (Weigert's hematoxylin, acid fuchsin, phosphomolybdic acid, and aniline blue) was used. To specifically identify collagen fibers and assess the degree of fibrosis in the dermis, a histochemical staining method with picosirius red (Mayer's hematoxylin, Sirius red F3BA, picric acid) was used. For the specific detection of cytoplasmic granules of mast cells in the dermis, a histochemical method of staining with Safranin-O, which binds to acidic proteoglycans and belongs to the group of basic stains, was used.

Morphometric analysis of micropreparations stained with hematoxylin and eosin was carried out in 10 randomly selected fields of view of a light microscope at ×400 magnification. Then, we calculated the thickness

of the epidermis, dermis, and hypodermis, the inner diameter of the hair follicle, and counting the number of hair follicles using a video microscopy system (Leica DM2000 microscope) and Leica Application Suite, Version 4.9.0 software. Computer morphometry was performed using the ImageJ computer image analysis system. The number of collagen fibers in the sections was measured using an image analysis computer program (BMI plus software, BumMi Universe Co.) and expressed as a percentage of the area occupied by collagen fibers in the upper dermis.

The number of mast cells after staining with safranin was determined by computer morphometry in 10 fields of view with a total area of 1.6 mm<sup>2</sup>, then the quantitative density of mast cells per 1 mm<sup>2</sup> was calculated by the formula:

$$\text{Nmast cells per 1 mm}^2 = \frac{\sum \text{Nmast cells} \times 1,000,000 \mu\text{m}^2}{\text{N fields of view} \times \text{S of one field} (\mu\text{m}^2)}$$

where  $\sum$ Nmast cells—the total number of mast cells in all studied fields.

Morphometric evaluation after histochemical staining according to Masson and Picosirius red, and immunohistochemistry (IHC) staining for type I and III collagen fibers was converted into points, taking into account the area and optical density (chromogeneity) in relative units: "1"—weak (0–0.3); "2"—moderate (0.3–0.6); and "3"—pronounced (>0.6).

**Immunohistochemical study**

Skin fragments after fixation for immunohistochemical analysis were prepared according to the standard protocol. Characteristics of antibodies are presented in Table 2. Cell nuclei were counterstained with Mayer's hematoxylin. The number of immunopositive cells was counted by three blinded pathologists in 10 randomly selected fields of view at ×400 magnification (in %). The number of collagen fibers in the sections was measured using an image analysis computer program (BMI plus

**Table 2.** Primary and secondary antibodies for immunohistochemistry.

	Manufacturer	Clone	Dilution	Country
<b>Primary antibodies</b>				
Monoclonal to Ki-67	ThermoFisher	MM1	1:100	USA
Monoclonal to p53	ThermoFisher	DO-7	1:100	USA
Monoclonal to Caspase 3	ThermoFisher	74T2	1:500	USA
Monoclonal to Collagen-I	ThermoFisher	COL-1	1:200	USA
Monoclonal to Collagen-III	ThermoFisher	FH-7A	1:50	USA
Polyclonal antibodies to IL-1 beta	ThermoFisher	–	1:100	USA
Polyclonal antibodies to IL-4	ThermoFisher	–	1:100	USA
Polyclonal antibodies to IL-6	ThermoFisher	–	1:100	USA
Polyclonal antibodies to IL-10	ThermoFisher	–	1:100	USA
<b>Secondary antibodies</b>				
HiDef Detection™ HRP Polymer system	Cell Marque	–	–	USA

software, BumMi Universe Co.) and expressed as a percentage of the area occupied by collagen fibers in the upper dermis. Stained sections were scored using a modified numerical scale from 0 to 3 (Abramov *et al.*, 2007). Microscopic analysis was performed using a video microscopy system (microscope Leica DM2000, Germany; camera Leica ICC50 HD).

#### **Statistical analysis**

All quantitative data were tested for normality. Under normal distribution, the group arithmetic mean (M) and SE/SD were calculated using the Microsoft Excel data analysis package (version 14.0.4760.1000, 32-bit). The data of immunohistochemical and morphometric studies obtained as a result of the calculation were processed using the computer program SPSS 12 for the Windows statistical software package (IBM Analytics, USA). Comparisons were made using analysis of variance.  $p$ -value  $<0.05$  was considered statistically significant.

#### **Ethical approval**

All manipulations were carried out in accordance with the International recommendations (EEC, Strasbourg, 1985), the European Convention for the Protection of Vertebrate Animals (EEC, Strasbourg, 1986), the Guidelines for Biomedical Research on the Care and Use of Laboratory Animals (ILAR, DELS), the Rules of laboratory practice and the Declaration of Helsinki (1964). The study was approved by the local ethics committee of the National Medical Research Radiological Centre №6 dated 04.12.2021.

### **Results**

No significant differences in body weight were found between control and experimental animals. As the animals grew older, body weight increased: by the third month of the experiment, weight gain was 67.3% in the control group, 73.7% in the group of single electron irradiation at a dose of 8 Gy, and 66.5% at a dose of 40 Gy and in the group of fractional electron irradiation—74.0%.

#### **Assessment of the skin of rats according to the RTOG (acute) and RTOG/EORTC (late) radiation morbidity scoring criteria**

##### **Macroscopic analysis**

The skin of the outer surface of the thigh in all animals of the control group remained unchanged, smooth, and retained its physiological color (whitish color) and short hairline. On the 10th day in group II, the skin also had a short hairline; in this group (85%), dry flaking was observed—the formation of white epidermal plates, corresponding to the initial signs of focal post-radiation dermatitis (RTOG—1 point). In group III, most animals (80%) showed a change in the physiological color of the skin to pink (redness), a sharp decrease in the density of the hairline, as well as moderate signs of post-radiation dermatitis (local moist peeling, moderate swelling) (RTOG—2 points). The skin of the majority (70%) of animals in group

IV, upon visual assessment, had a bright pink color with a bluish tinge and areas of sparse and short hair, merging moist peeling and pronounced edema, which corresponds to the signs of pronounced exudative post-radiation dermatitis with slight local restoration of the hairline (RTOG—3 points).

The skin of the outer surface of the thighs of the control animals did not visually differ from that in the second week of the experiment. In group II, in the skin of most animals (90%), 3 months after irradiation, slight atrophy, increased pigmentation, focal hair loss, thickening and thinning of subcutaneous fat were observed; one animal (10%) showed no signs of delayed post-radiation skin lesions (RTOG/EORTC—1 point). A visual assessment of the skin of group III after 3 months revealed: baldness of the outer surface of the thigh, redness, moderate induration, and contracture (up to 10% of the area) of the subcutaneous fat in 8 out of 10 animals (80%) (RTOG/EORTC—2 points). In the vast majority of cases (90%), after fractional local irradiation with electrons in a total dose of 78 Gy, pronounced skin atrophy and total induration of subcutaneous fat were observed, the contracture of which occupied more than 10% of the area (RTOG/EORTC—3 points).

#### **Morphological, histochemical, and morphometric analysis**

##### **Control**

The skin in the control group consisted of the epidermis, papillary and reticular dermal layers, and hypodermis, skin appendages, and abundant hair follicles were clearly visualized (Figs. 1A and 2).

##### **Single 8 Gy irradiation**

##### **Microscopic analysis**

A thickening of the epidermal basal layer in the hair follicles region with slight delamination of the stratum corneum and intact appendages, focal leukocyte infiltration, perivascular edema in the dermal papillary layer, and dilated blood vessels with erythrocyte sludge was noted 10 days after 8 Gy single local electron irradiation (Table 3). Three months after a single irradiation at a dose of 8 Gy we observed complete recovery of the studied morphometric characteristics of the skin and its appendages (Table 4).

##### **Histochemical analysis**

According to Masson and safranin staining the skin after 10 days after 8 Gy electron irradiation practically did not differ from the control group (Table 5). Then, we performed a morphometric study of the skin stained with picosirius red and visualized in polarized light. Ten days after a single 8 Gy irradiation, we found a slight decrease in the average density of types I and III collagen fibers compared to the control (Fig. 3).

Three months after 8 Gy electron irradiation, the skin of the outer surface of the thigh showed an almost complete restoration of the histoarchitectonics of the epidermis and dermis with weak staining of the fibers and a small number of mast cells. The parameters of

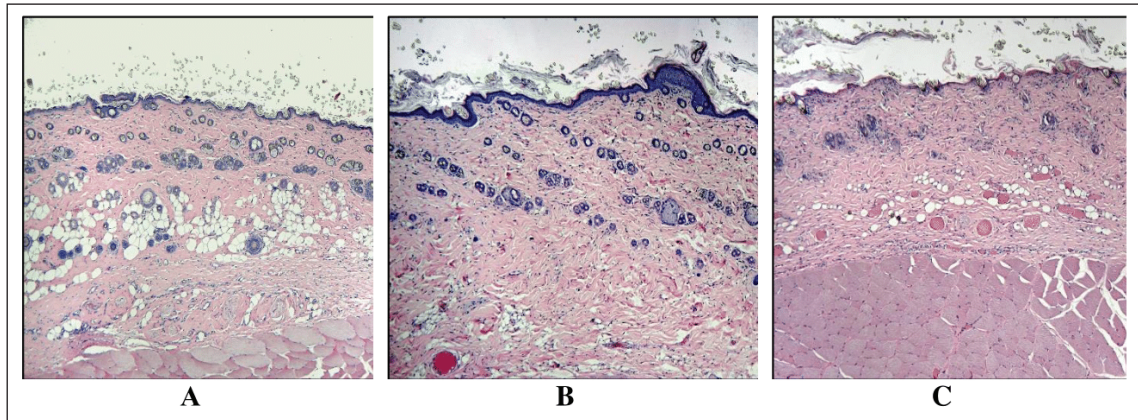


**Fig. 1.** Fragments of the skin of the control group on the 10th day of the experiment (A), as well as 10 days (B) and 3 months (C) after a single local irradiation with electrons at a dose of 40 Gy. H&E stain, magn.  $\times 100$ .

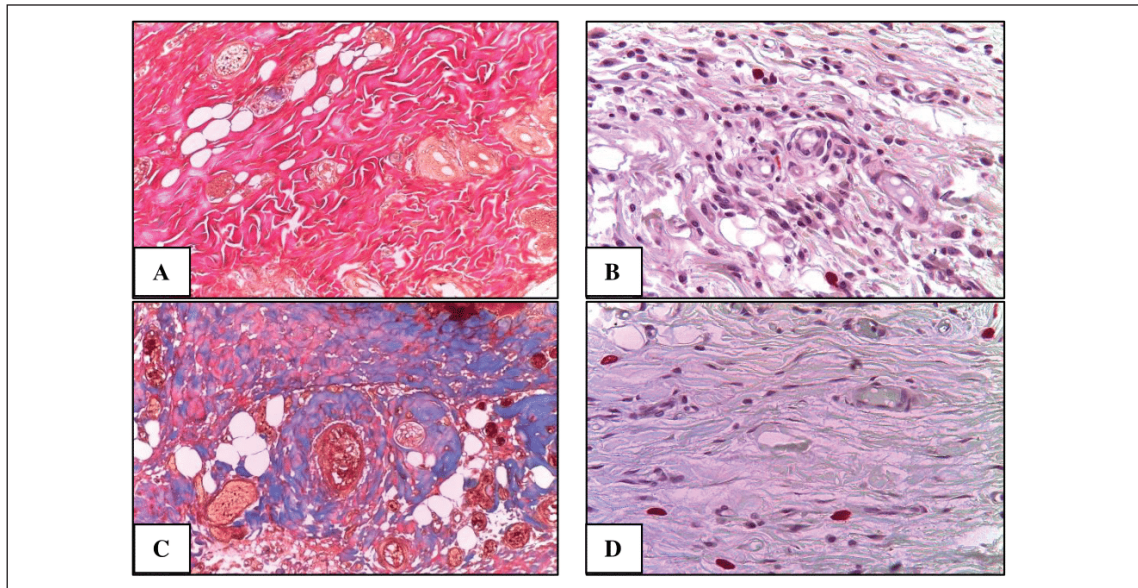


**Fig. 2.** Fragments of the skin of the control group (A, B) and 10 days after fractional irradiation (C, D). A, C—staining according to Masson; B, D—staining with safranin. Magn.  $\times 200$ .

**Table 3.** Morphometric parameters of the epidermis and dermis 10 days after electron irradiation at different doses.

Group	Epidermis thickness, $\mu\text{m}$ M $\pm$ SD	Dermis thickness, $\mu\text{m}$ M $\pm$ SD	Hypodermis thickness, $\mu\text{m}$ M $\pm$ SD	Internal diameter of the hair follicle, $\mu\text{m}$ M $\pm$ SD	Number of hair follicles, in 1 $\text{mm}^2$ M $\pm$ SD
Control	22.7 $\pm$ 1.1	381.8 $\pm$ 19.0	378.7 $\pm$ 18.8	36.5 $\pm$ 1.8	40.9 $\pm$ 2.0
Single irradiation, 8 Gy	11.2 $\pm$ 0.5 <sup>a</sup>	320.6 $\pm$ 15.8 <sup>a</sup>	148.2 $\pm$ 7.3 <sup>a</sup>	23.4 $\pm$ 1.1 <sup>a</sup>	37.3 $\pm$ 1.8 <sup>a</sup>
Single irradiation, 40 Gy	4.1 $\pm$ 0.2 <sup>b</sup>	223.9 $\pm$ 11.1 <sup>b</sup>	84.6 $\pm$ 4.1 <sup>b</sup>	9.5 $\pm$ 0.4 <sup>b</sup>	31.6 $\pm$ 1.5 <sup>b</sup>
Fractional irradiation, 78 Gy	—	901.2 $\pm$ 44.9 <sup>c</sup>	518.7 $\pm$ 25.8 <sup>c</sup>	—	—

<sup>a</sup>control versus 8 Gy (single dose), <sup>b</sup>control versus 40 Gy (single dose), and <sup>c</sup>control versus 78 Gy (fractional);  $p < 0.05$ .

**Table 4.** Morphometric parameters of the epidermis and dermis 3 months after electron irradiation at different doses.

Group	Epidermis thickness, $\mu\text{m}$ M $\pm$ SD	Dermis thickness, $\mu\text{m}$ M $\pm$ SD	Hypodermis thickness, $\mu\text{m}$ M $\pm$ SD	Internal diameter of the hair follicle, $\mu\text{m}$ M $\pm$ SD	Number of hair follicles, in 1 $\text{mm}^2$ M $\pm$ SD
Control	22.2 $\pm$ 1.0	388.1 $\pm$ 18.7	363.4 $\pm$ 18.3	38.2 $\pm$ 1.5	36.4 $\pm$ 1.6
Single irradiation, 8 Gy	20.1 $\pm$ 0.9 <sup>a</sup>	376.3 $\pm$ 17.5 <sup>a</sup>	334.6 $\pm$ 16.1 <sup>a</sup>	33.6 $\pm$ 1.4 <sup>a</sup>	32.1 $\pm$ 1.5 <sup>a</sup>
Single irradiation, 40 Gy	11.7 $\pm$ 0.5 <sup>b</sup>	332.6 $\pm$ 16.1 <sup>b</sup>	275.8 $\pm$ 13.7 <sup>b</sup>	32.9 $\pm$ 1.5	22.6 $\pm$ 1.1 <sup>b</sup>
Fractional irradiation, 78 Gy	4.9 $\pm$ 0.2 <sup>c</sup>	571.2 $\pm$ 27.2 <sup>c</sup>	468.3 $\pm$ 23.1 <sup>c</sup>	–	–

<sup>a</sup>control versus 8 Gy (single dose), <sup>b</sup>control versus 40 Gy (single dose), and <sup>c</sup>control versus 78 Gy (fractional);  $p < 0.05$ .

**Table 5.** The number of mast cells (in 1  $\text{mm}^2$ ) and the density of the fibrous component (in points) in the dermis on day 10 in the control and experimental groups.

Group	Mast cells, M $\pm$ S D	Fibrous component, M $\pm$ SD
Control	22.5 $\pm$ 1.1	1.7 $\pm$ 0.07
Single irradiation, 8 Gy	30.2 $\pm$ 1.4 <sup>a</sup>	2.0 $\pm$ 0.09 <sup>a</sup>
Single irradiation, 40 Gy	36.6 $\pm$ 1.7 <sup>b</sup>	2.3 $\pm$ 0.11 <sup>b</sup>
Fractional irradiation, 78 Gy	48.4 $\pm$ 2.3 <sup>c</sup>	2.6 $\pm$ 0.12 <sup>c</sup>

<sup>a</sup>control versus 8 Gy (single dose), <sup>b</sup>control versus 40 Gy (single dose), and <sup>c</sup>control versus 78 Gy (fractional);  $p < 0.05$ .

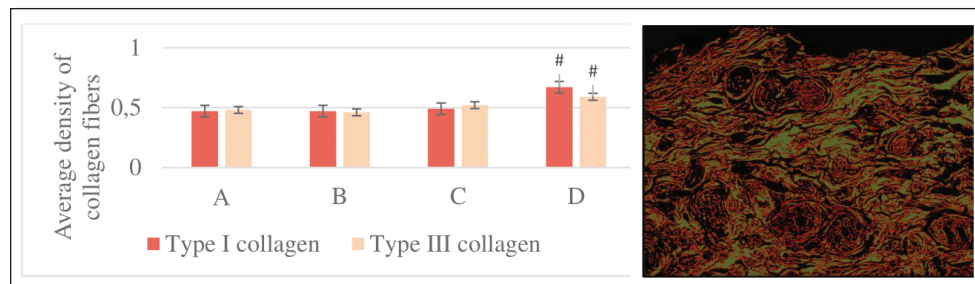


**Fig. 3.** The average density of types I and III collagen fibers in the skin after 10 days (left). A–control; B–single irradiation, 8 Gy; B–single irradiation, 40 Gy; G–fractional, 78 Gy. #–significant difference ( $p < 0.05$ ) compared to the control. Group IV dermis stained with picrosirius red in polarized light (type I collagen—red glow, type III collagen—green glow), magn.  $\times 200$  (right).

this group did not significantly differ from the control dermis (Fig. 4).

#### Single 40 Gy irradiation

##### Microscopic analysis

Flattening and partial absence of the epidermal basal layer, smoothed dermal papillary layer, dilated blood vessels with erythrocyte sludge, absence of sebaceous glands, intact hair follicles, and subcutaneous fat was noted in group III 10 days after 40 Gy single local electron irradiation. Microcavities of the epidermal-dermal junction, filled with desquamated epidermal cells and polymorphonuclear leukocytes were found (Table 3, Fig. 1B). Three months after a single irradiation at a dose of 40 Gy, we observed partial

recovery of the studied morphometric characteristics of the skin and its appendages (Table 4, Fig. 1C).

##### Histochemical analysis

According to Masson and safranin staining, we have found that 40 Gy electron irradiation results in moderate outgrowth of the fibrous component of predominantly the papillary dermis (Table 5). Then, we performed a morphometric study of the skin stained with picrosirius red and visualized in polarized light. 10 days after 40 Gy, there was an increase in this indicator compared to the control (Fig. 3). A 40 Gy dose after 3 months led to an increase in the number of mast cells and the density of the fibrous component compared to the control (Fig. 4).

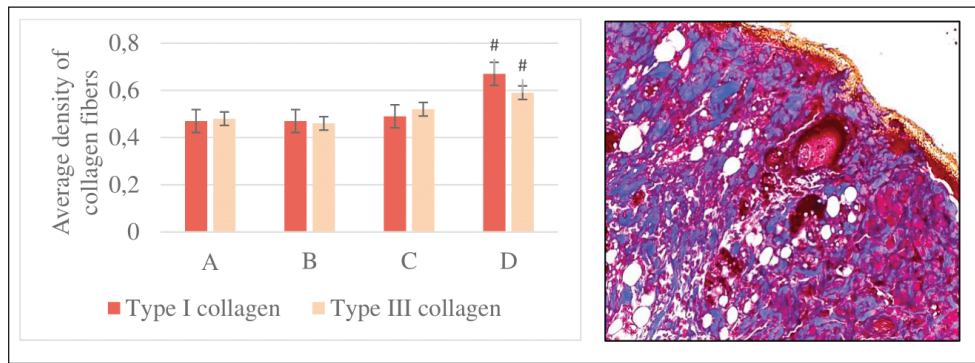


**Fig. 4.** The average density of types I and III collagen fibers in the skin after 3 months (left). A–control; B–single irradiation, 8 Gy; C–single irradiation, 40 Gy; D–fractional, 78 Gy. #–significant difference ( $p < 0.05$ ) compared to the control. Group IV skin fragment 3 months after 78 Gy fractional irradiation. Masson stain, magn.  $\times 200$  (right).

### Fractionation 78 Gy

#### Microscopic analysis

The epithelium is partially absent, the dermal papillary layer is smoothed and intensely infiltrated with polymorphonuclear leukocytes, edema of the dermal reticular layer and hypodermis, collagen fibers are loosened, dilated blood vessels with endothelial detachment, aggregation, and sludge of erythrocytes were noted 10 days after 78 Gy fractional local electron irradiation, as well as the sebaceous glands and hair follicles, are destructured (Table 3). After 3 months fractional irradiation led to the growth of the connective tissue component of the skin with signs of RIF: a pronounced thickening of the dermis and hypodermis, the absence of hair follicles, and the complete or partial absence of sebaceous and sweat glands (single preserved glands are strongly destructured). Compared with the results of a morphometric assessment of the skin of the same group (IV) after 10 days, there was a weak restoration of the epidermis, a slight decrease in the thickness of the dermis (by 36.6%), and hypodermis (by 9.8%) (Table 4).

#### Histochemical analysis

According to Masson and safranin staining, fractional electron irradiation led to a pronounced increase in the volume of connective tissue in the papillary and reticular layers of the skin when stained according to Masson. The epidermis was almost completely absent in this group (Table 5, Fig. 2). Then, we performed a morphometric study of the skin stained with picrosirius red and visualized in polarized light. On the 10th day, fractional irradiation resulted in a statistically significant increase in the average density of both types of collagen fibers (especially type III) compared to the control (Fig. 3).

At the same time, the morphological pattern of post-radiation fibrosis with Masson skin staining was observed after fractional electron irradiation at a total 78 Gy dose. In addition, it led to a statistically

significant increase in the average density of types I and III collagen fibers compared to the control, with type I collagen being more actively expressed in the dermis (Fig. 4).

Thus, the results of a morphometric study of the skin with the determination of the average density of types I and III collagen fibers were obtained, which reliably confirm the assumption of the induction of RIF in the long term (3 months) after fractional electron irradiation. Nevertheless, the changes in this parameter after a single electron irradiation were not statistically significant and approached the control values.

#### Immunohistochemical study

##### Assessment of proliferation and apoptosis of keratinocytes

Immunostaining of the control skin for the proliferation protein Ki-67, the apoptosis termination phase protein Caspase-3, and the proapoptotic protein p53 was localized in the keratinocytes of the basal layer and in the interfollicular epitheliocytes. Immunoreactivity of Ki-67 10 days after electron irradiation showed a dose-proportional decrease in the number of IHC-positive keratinocytes in all experimental groups compared to the control. Three months after the 8 Gy dose, the immunoreactivity of this factor did not differ from the control. After 40 Gy, it was slightly higher than in the control. At the same time, after fractional irradiation, it was 2.1 times lower than in the control. An increase in the intensity of keratinocyte apoptosis after electron irradiation was confirmed by a directly proportional increase in Caspase-3 immunoreactivity. Three months after 8 Gy of single irradiation, we observed the restoration of the immunoreactivity level of this protein to control values. After a 40 Gy dose, we found it increased by 2.46 times compared to the control. At the same time, fractional irradiation led to the maintenance of high immunoreactivity levels of this marker after 3 months. Similar immunohistochemical patterns were found when epidermis and dermis were stained with

antibodies to the proapoptotic p53 protein (Table 6, Fig. 5).

**Assessment of the condition of the fibrous component of the skin**

The intensity of immunoreactivity of types I and III collagens in the dermis is directly correlated with the dose of electron irradiation, the timing of development, and the degree of post-radiation damage. Ten days after single electron irradiation in the dermis, insignificant changes in the immunoreactivity of type I collagen and an increase in the immunoreactivity of type III collagen were observed compared to the control. Fractional irradiation, after 10 days, led to the growth of the fibrous component of the dermis, which was confirmed by the immunoreactivity levels of both types of collagen

fibers. It is important to note that the immunoreactivity of type III collagen predominated at this time.

Three months after 8 Gy of single irradiation, the expression levels of types I and III collagens were restored. This confirms the reversibility of post-radiation skin damage in this group. On the contrary, fractional electron irradiation led to the preservation of high immunoreactivity values of collagen fibers with a predominance of type I collagen. This is a sign of the development of RIF, as the most common complication of radiotherapy (Table 7, Fig. 6).

**Evaluation of the inflammatory response of the skin**

An immunohistochemical study revealed pro-inflammatory (IL-1 $\beta$  and IL-6) and anti-inflammatory cytokines (IL-4 and IL-10) in keratinocytes of the basal layer of the epidermis and inflammatory cells of the

**Table 6.** Expression of proliferation and apoptosis factors in the skin of the control and experimental groups (M  $\pm$  SD), %.

Group	Ki-67		Caspase 3		p53	
	Day 10	3 months	Day 10	3 months	Day 10	3 months
Control	37.2 $\pm$ 1.8	33.7 $\pm$ 1.6	5.4 $\pm$ 0.2	5.9 $\pm$ 0.2	7.8 $\pm$ 0.3	7.6 $\pm$ 0.3
Single irradiation, 8 Gy	31.8 $\pm$ 1.6 <sup>a</sup>	32.5 $\pm$ 1.5	18.6 $\pm$ 0.9 <sup>a</sup>	5.7 $\pm$ 0.2	23.5 $\pm$ 1.1 <sup>a</sup>	8.1 $\pm$ 0.4
Single irradiation, 40 Gy	14.5 $\pm$ 0.7 <sup>b</sup>	38.6 $\pm$ 1.4 <sup>b</sup>	35.5 $\pm$ 1.7 <sup>b</sup>	14.5 $\pm$ 0.7 <sup>b</sup>	41.2 $\pm$ 2.0 <sup>b</sup>	12.7 $\pm$ 0.6 <sup>b</sup>
Fractional irradiation, 78 Gy	6.3 $\pm$ 0.3 <sup>c</sup>	16.1 $\pm$ 0.6 <sup>c</sup>	62.4 $\pm$ 3.1 <sup>c</sup>	73.2 $\pm$ 3.6 <sup>c</sup>	57.2 $\pm$ 2.8 <sup>c</sup>	64.3 $\pm$ 3.2 <sup>c</sup>

<sup>a</sup>control versus 8 Gy (single dose), <sup>b</sup>control versus 40 Gy (single dose), and <sup>c</sup>control versus 78 Gy (fractional); *p* < 0.05.

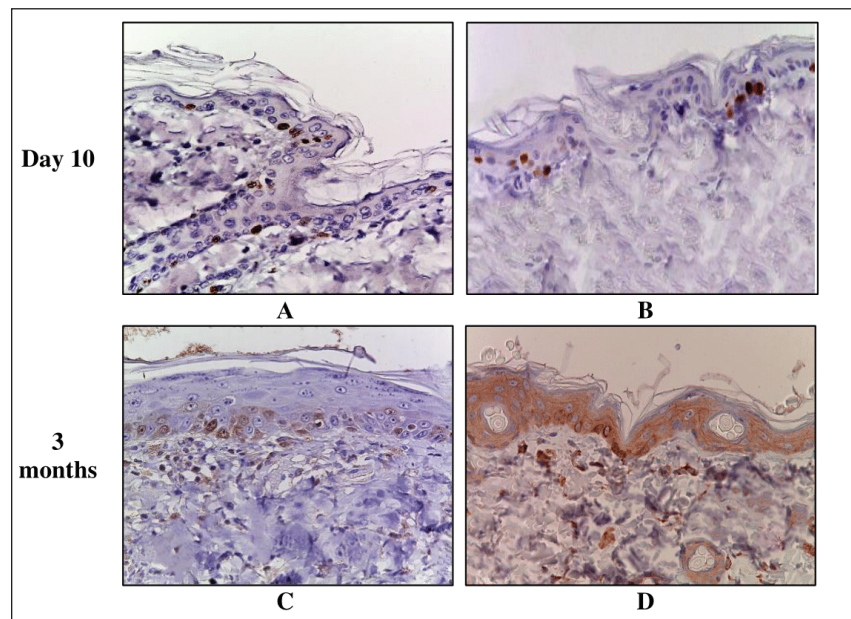


**Fig. 5.** Skin of the control and experimental groups after 10 days and 3 months. A—control group, immunohistochemical reaction with antibodies to Ki-67; B—after 8 Gy single electron irradiation, immunohistochemical reaction with antibodies to Caspase-3; C—after 40 Gy single electron irradiation, immunohistochemical reaction with antibodies to Ki-67; D—after 40 Gy single electron irradiation, immunohistochemical reaction with antibodies to Caspase-3. Nuclei were stained with hematoxylin. Magn.  $\times$ 400.



**Table 7.** Scoring of the expression of types I and III collagen fibers in the skin of the control and experimental groups.

Group	Type I collagen M ± SE		Type III collagen M ± SE	
	Day 10	3 months	Day 10	3 months
Control	1.3 ± 0.05	1.4 ± 0.06	1.4 ± 0.06	1.4 ± 0.06
Single irradiation, 8 Gy	1.2 ± 0.06*	1.5 ± 0.06*	1.5 ± 0.05*	1.4 ± 0.05*
Single irradiation, 40 Gy	1.5 ± 0.06*	1.7 ± 0.08*	1.8 ± 0.05*	1.5 ± 0.06*
Fractional irradiation, 78 Gy	1.8 ± 0.1*	2.4 ± 0.11*	2.1 ± 0.07*	1.9 ± 0.08*

\*Significant difference compared to control,  $p < 0.05$ .

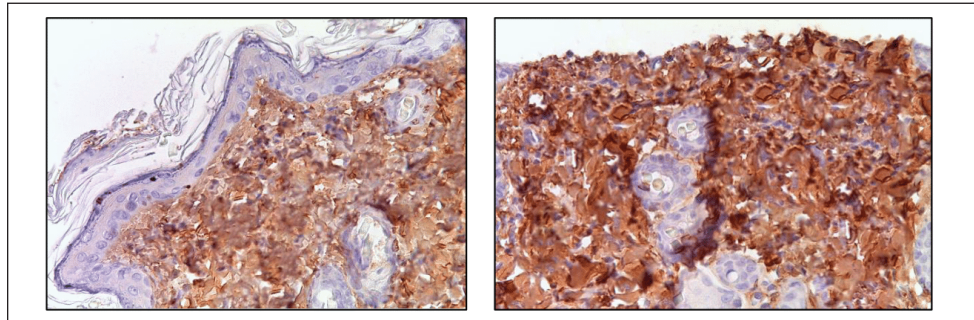


**Fig. 6.** Skin fragments 3 months after a 40 Gy single (left) and fractional (right) local electron irradiation. Immunohistochemical reaction with antibodies to Collagen I; nuclear staining with hematoxylin. Magn. ×400.

dermis of the control group. Ten days after 8 Gy and 40 Gy single electron irradiation, a dose-dependent increase in the expression levels of both pro- and anti-inflammatory cytokines was noted compared to the control. After fractional electron irradiation, we found an imbalance of markers of the inflammatory response. High expression levels of IL-1 $\beta$  and IL-6 were accompanied by a sharp decrease in the expression levels of IL-4 and IL-10 compared to the control (Fig. 7).

Three months after 8 Gy of local electron irradiation, we observed a return of the immunoreactivity levels of pro-inflammatory and anti-inflammatory cytokines to the control values. At the same time, after 40 Gy irradiation, we observed a slight increase in the expression of pro-inflammatory cytokines and IL-4. Three months after fractional electron irradiation, elevated immunoreactivity levels of IL-1, IL-6 (including in single fibroblast cells), and IL-4 remained. In addition, this was accompanied by a slight increase in the level of IL-10 immunoreactivity compared to the control (Fig. 7).

### Discussion

This study is devoted to the immunohistochemical evaluation of impaired keratinocyte proliferation, skin collagen synthesis, the degree of RIF, and the expression of inflammatory cytokines after 8 Gy and

40 Gy single local electron irradiation and 78 Gy fractional local electron irradiation.

Radiation therapy is based on the concept that actively proliferating abnormal cells are more sensitive to ionizing radiation and cannot regenerate as efficiently as healthy ones. During a few hours there are formation of DNA double-strand breaks (direct effect), reactive oxygen species (ROS), and other radicals that damage DNA and other cellular components (for example, cell membranes, proteins, and lipids; indirect effect) (Jackson and Bartek, 2009; Mehta *et al.*, 2010; Yoshimura *et al.*, 2013). Cell death occurs by apoptosis or necrosis with the release of damage-associated molecular patterns: heat shock proteins, HMGB1, hyaluronan fragments, and so on (Lumniczky and Sáfrány, 2015; Brix *et al.*, 2017).

Some authors noted the death of keratinocytes in the epidermal basal layer after 3–5 Gy single  $\gamma$ -irradiation (Ward *et al.*, 1990; Ran *et al.*, 2004). However, in our study, an 8 Gy single local electron irradiation leads to weak epidermal pathomorphological changes. A slight decrease in the density of collagen fibers found after 8 Gy single local electron irradiation is also explained by the relatively low damaging ability of this dose (Soref and Fahl, 2015), at which microscopic analysis of the skin showed only a partial thickening of the basal layer and delamination of the stratum corneum of the epidermis. At the same time, the dermis remained intact, which explains the absence of differences in collagen

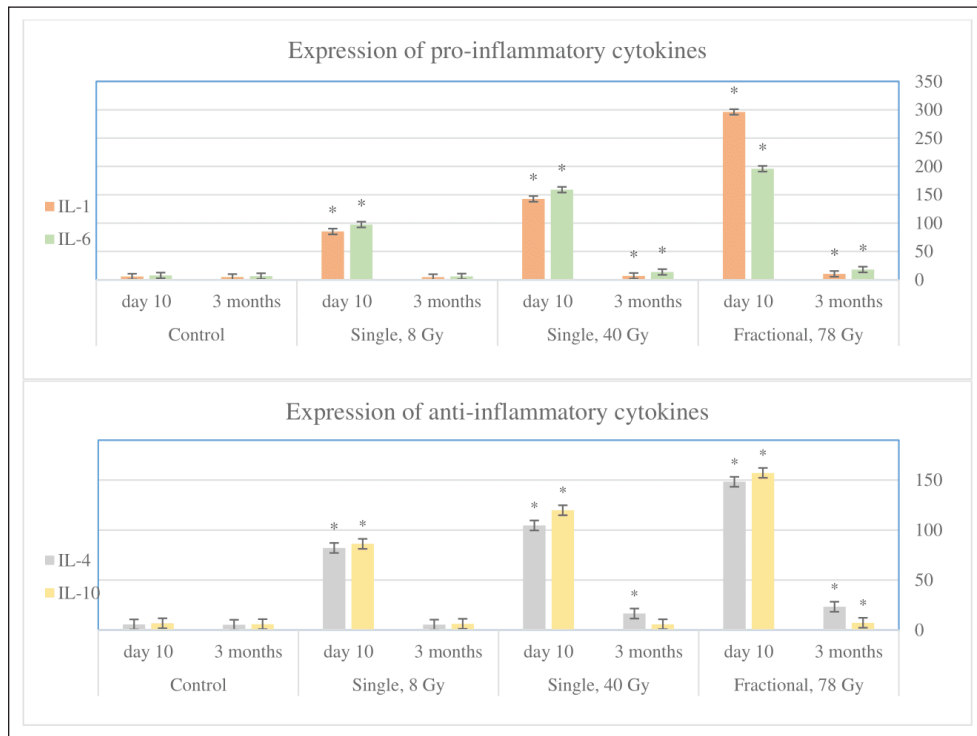


**Fig. 7.** The number of inflammatory cells expressing pro- (IL-1 and IL-6) and anti-inflammatory (IL-4 and IL-10) cytokines in 1 mm<sup>2</sup> of the skin of the control and experimental groups after 10 days and 3 months. \* significant differences compared to the control.

metabolism in this group compared to the control, since most of the collagen fibers and fibroblasts that produce them are located mainly in the papillary dermis (Blair *et al.*, 2020).

A decrease in the density of microvessels in the skin, leading to tissue ischemia and, thereby, significantly reducing the rate of wound healing after 25 Gy X-irradiation was found in another study. In addition, the authors noted an increase in the expression of pro-inflammatory cytokines (TNF- $\alpha$ , IL-1, and IL-6), the release of cell adhesion molecules, which accelerated the migration, adhesion, and exudation of leukocytes and induced the migration of macrophages, neutrophils, and monocytes, which leads to a local inflammatory response to radiation injury (Li *et al.*, 2022). The polymorphonuclear infiltration of the skin found at various doses of single local electron irradiation can be explained by a similar mechanism the development of inflammation, the key role which is played by the imbalance of pro-inflammatory and anti-inflammatory cytokines. These changes in the inflammatory response are most pronounced after fractional local electron irradiation. Thus, immunohistochemical analysis showed an increase in both pro-inflammatory (IL-1 and IL-6) and anti-inflammatory (IL-4 and IL-10) cytokines after 8 Gy single local electron irradiation. This was also more pronounced after 40 Gy single local

electron irradiation; however, the balance of cytokines was preserved. Thus, probably that damage after 8 Gy and 40 Gy is compensated and can be repaired, and after 78 Gy irradiation decompensation occurs. Pro-inflammatory cytokines predominate over anti-inflammatory cytokines. Disruption of compensatory defense systems also occurs and all these changes lead to the development of unreparable acute [radiation-induced dermatitis, (RID)] and late (radiation-induced skin fibrosis, RIF) post-radiation complications.

Some authors have noted necrosis of keratinocytes, which is pathogenetically associated with ischemia due to the destruction of the blood vessels, as well as damage to the sebaceous and sweat glands and hair follicles after 45 Gy photons irradiation (Wang *et al.*, 2013; McPartlin *et al.*, 2014). On the contrary, in our study hair follicles were preserved at all levels of the skin and the sebaceous glands were absent, probably due to their greater radiosensitivity after 40 Gy single local electron irradiation. This fact indirectly confirms the concept of a "light" effect of electron irradiation on the skin appendages.

In the study, the most pronounced skin damage was observed after electron fractions with minor damage to the vascular wall, while other types of irradiation (for example, photons, X- and  $\gamma$ -rays) at similar fractionation

doses led to its complete destruction (Olschewski *et al.*, 2006).

The molecular mechanisms of radiation-induced cell death are still poorly understood. The revealed imbalance between proliferation and apoptosis of keratinocytes, including those caused by irradiation, leads to Bcl-2 deactivation and p53 induction. This is accompanied by a decrease in the cell pool due to the modulation of glycogen synthase kinase-3 (GSK3-), extracellular signal-regulated kinase (ERK-), and Ras/Raf/MEK-1 signaling pathways (Wang *et al.*, 2006; Morel *et al.*, 2009).

A decrease in the number of Ki-67-positive keratinocytes, which is associated with the direct toxic effect of ionizing radiation on actively proliferating cells, in which the destruction of cell membranes and the structure of macromolecules (DNA, RNA, proteins, lipids, and so on), as well as modulation of MAPK, PI3K, and NF $\kappa$ B signaling pathways, proteins of the ErbB family, and disruption of cellular respiration at the level of the electron transport chain in mitochondria was observed after 8 Gy and 40 Gy. All these processes lead to an imbalance of the antioxidant and prooxidant systems (Reisz *et al.*, 2014). In addition, the observed inhibition of keratinocyte differentiation is associated with damage to such signaling pathways as: PI3-kinases/Akt and Ras/Raf/MEK-1, as well as GSK-3 and ERK (Wang *et al.*, 2006).

Modulation of the activity of the above cascades leads to chromatin condensation and DNA fragmentation, i.e., apoptosis, confirmed by an increase in the number of caspase-3- and p53-positive cells. Apoptosis is activated via extrinsic and intrinsic pathways and caspase-3 is responsible for the terminal phase. The cell cycle regulator is the proapoptotic protein p53, which also was increased.

It should be noted a decrease in the number of mitotically dividing generations of epidermal basal layer keratinocytes was observed after single electron irradiation (Martincorena *et al.*, 2015). Thus, the results of the IHC study showed a shift in the proliferative-apoptotic balance toward keratinocyte apoptosis, which is most pronounced in the fractional group compared to single electron irradiation (Reisz *et al.*, 2014). Therefore, unlike other types of ionizing radiation, electrons show the smallest depth of skin damage.

Many studies have reported skin fibrosis after inflammation in response to injury, thermal and chemical burns, and radiation. In turn, inflammation (RID) is described as a consequence of ionizing radiation, which contributes to the destruction of macromolecules and cell membranes with the formation of ROS, and oxidative stress develops. This leads to inflammatory infiltration and disruption of the connective tissue structure (i.e., a decrease in the density of collagen fibers) (Sultan *et al.*, 2011). For example, ROS destroys the endothelium of small-caliber blood vessels, triggering a cellular inflammation

(Yoshimura *et al.*, 2013). This leads to the activation of pro-inflammatory cytokines, an increase in the expression of which was found in all irradiated groups. However, in response to the ROS release an increase in antioxidant system enzymes has been reported, which aim to capture and destroy ROS, thereby reducing skin damage. The key role belongs to metalloproteinase-9, which is responsible for the remodeling of extracellular matrix components and is regulated by endogenous tissue inhibitors of metalloproteinases and TGF- $\beta$ 1, the relationship of which in the skin after irradiation has not been studied enough (da Silva Santin *et al.*, 2020). After the initial reaction to radiation damage, the cells of the extracellular matrix begin to regenerate the damaged structures. The production of collagen fibers, i.e., fibrosis is the most common outcome of this process. Moreover, in some cases, this process can probably proceed uncontrollably as a result of disruption of regulatory mechanisms after irradiation at high doses with total damage to the deep layers of the skin, which was confirmed by the results of our study after 78 Gy fractional electron irradiation (group IV) and partially after 40 Gy single electron irradiation (III group). This is consistent with the opinion of other authors (Riekki *et al.*, 2002).

According to the results of an immunohistochemical study, an increase in the dose and frequency of exposure led to hyperactivation of collagen synthesis due to the intensification of signaling pathways, probably responsible for fibrosis (Borrelli *et al.*, 2019). In our study, an increase in immunolabeling for type I and III collagen fibers in skin fragments after high doses of single local electron irradiation was revealed, and 78 Gy fractional irradiation led to the most active production of collagen fibers, the density of which in this group was significantly higher compared to the control. This result of electron irradiation is called RIF (Borrelli *et al.*, 2019).

After 8 Gy single local electron irradiation, the risk of developing RIF is minimal, since the deep layers of the skin, in which fibroblasts are located and collagen fibers are synthesized, remain intact with a high degree of probability. However, according to the results of histological and immunohistochemical studies, an intensification of inflammation and collagen formation and signs of skin RIF as an outcome of RID with an increase in the radiation dose was observed. They were most pronounced in the fractional electron irradiation group and an important role was played by the destruction of the skin-deep layers with a violation of the regulation of collagenogenesis. Probably, it was also related to the duration of the impact of the damaging factor.

Thus, 8 Gy and 40 Gy single local electron irradiation leads to a shift in the proliferative-apoptotic balance of keratinocytes toward their apoptosis, the activity of which is directly correlated with the dose of ionizing radiation, and 78 Gy summary dose in fractions

leads to partial desquamation of the epithelium and inflammatory infiltration. In addition, after 3 months a significant increase in the expression of type I and III collagen fibers and the development of radiation-induced skin fibrosis takes place against the background of 78 Gy fractional local electron irradiation. At the same time, after single 8 Gy and 40 Gy electron irradiation, the described immunohistochemical changes were insignificant and directly correlated with the dose of ionizing radiation.

#### Acknowledgment

None.

#### Conflict of interest

All authors declare that there is no conflict of interest.

#### Funding

This research received no specific grant.

#### Author contributions

The concept and design of the study: G.A.D., S.N.K., Ye.Yu.Sh, P.V.Sh., A.D.K. Collection and processing of material: A.Kh.M., M.A.V., L.N.A., M.V.F. Statistical processing: S.N.K., M.A.V., N.A.G. Text writing: G.A.D., A.Kh.M., M.A.V., L.N.A., N.A.G. Editing: G.A.D., M.V.F., Ye.Yu.Sh, P.V.Sh., A.D.K.

#### Data availability

All data supporting the findings of this study are available within the manuscript.

#### References

- Abramov, Y., Golden, B. and Sullivan, M. 2007. Histologic characterization of vaginal vs. abdominal surgical wound healing in a rabbit model. *Wound Repair. Regen.* 15(1), 80–86.
- Blair, M.J., Jones, J.D., Woessner, A.E. and Quinn, K.P. 2020. Skin structure-function relationships and the wound healing response to intrinsic aging. *Adv. Wound. Care.* 9(3), 127–143.
- Borrelli, M.R., Shen, A.H., Lee, G.K., Momeni, A., Longaker, M.T. and Wan, D.C. 2019. Radiation-induced skin fibrosis: pathogenesis, current treatment options, and emerging therapeutics. *Ann. Plast. Surg.* 83(4S Suppl. 1), S59–S64.
- Brix, N., Tiefenthaler, A., Anders, H., Belka, C. and Lauber, K. 2017. Abscopal, immunological effects of radiotherapy: narrowing the gap between clinical and preclinical experiences. *Immunol. Rev.* 280(1), 249–279.
- Chua, B., Jackson, J.E., Lin, C. and Veness, M.J. 2019. Radiotherapy for early non-melanoma skin cancer. *Oral. Oncol.* 98, 96–101.
- Cives, M., Mannavola, F., Lospalluti, L., Sergi, M.C., Cazzato, G., Filoni, E., Cavallo, F., Giudice, G., Stucci, L.S., Porta, C. and Tucci, M. 2020. Non-melanoma skin cancers: biological and clinical features. *Int. J. Mol. Sci.* 21(15), 5394.
- da Silva Santin, M., Koehler, J., Rocha, D.M., Dos Reis, C.A., Omar, N.F., Fidler, Y., de Miranda Soares, M.A. and Gomes, J.R. 2020. Initial damage produced by a single 15-Gy x-ray irradiation to the rat calvaria skin. *Eur. Radiol. Exp.* 4(1), 32.
- Jackson, S.P. and Bartek, J. 2009. The DNA-damage response in human biology and disease. *Nature* 461(7267), 1071–1078.
- Li, Z., Gan, H., Liang, A., Wang, X., Hu, X., Liang, P., Xu, G., Huang, Q., Li, J. and Li, H. 2022. Promoting repair of highly purified stromal vascular fraction gel combined with advanced platelet-rich fibrin extract for irradiated skin and soft tissue injury. *Ann. Transl. Med.* 10(17), 933.
- Lumniczky, K. and Sáfrány, G. 2015. The impact of radiation therapy on the antitumor immunity: local effects and systemic consequences. *Cancer. Lett.* 356(1), 114–125.
- Martincorena, I., Roshan, A., Gerstung, M., Ellis, P., Van Loo, P., McLaren, S., Wedge, D.C., Fullam, A., Alexandrov, L.B., Tubio, J.M., Stebbings, L., Menzies, A., Widaa, S., Stratton, M.R., Jones, P.H. and Campbell, P.J. 2015. Tumor evolution. High burden and pervasive positive selection of somatic mutations in normal human skin. *Science* 348(6237), 880–886.
- McPartlin, A.J., Slevin, N.J., Sykes, A.J. and Rembielak, A. 2014. Radiotherapy treatment of non-melanoma skin cancer: a survey of current UK practice and commentary. *Br. J. Radiol.* 87(1043), 20140501.
- Mehta, S.R., Suhag, V., Semwal, M. and Sharma, N. 2010. Radiotherapy: basic concepts and recent advances. *Med. J. Armed. Forces. India.* 66(2), 158–162.
- Morel, C., Carlson, S.M., White, F.M. and Davis, R.J. 2009. Mcl-1 integrates the opposing actions of signaling pathways that mediate survival and apoptosis. *Mol. Cell. Biol.* 29(14), 3845–3852.
- Müller, K. and Meineke, V. 2007. Radiation-induced alterations in cytokine production by skin cells. *Exp. Hematol.* 35(4 Suppl. 1), 96–104.
- Olschewski, T., Bajor, K., Lang, B., Lang, E. and Seegenschmiedt, M.H. 2006. Radiotherapy of basal cell carcinoma of the face and head: importance of low dose per fraction on long-term outcome. *J. Dtsch. Dermatol. Ges.* 4(2), 124–130.
- Pashazadeh, A., Boese, A. and Friebe, M. 2019. Radiation therapy techniques in the treatment of skin cancer: an overview of the current status and outlook. *J. Dermatol. Treat.* 30(8), 831–839.
- Perez, M., Abisaad, J.A., Rojas, K.D., Marchetti, M.A. and Jaimes, N. 2022. Skin cancer: primary, secondary, and tertiary prevention. Part I. *J. Am. Acad. Dermatol.* 87(2), 255–268.
- Ran, X., Cheng, T., Shi, C., Xu, H., Qu, J., Yan, G., Su, Y., Wang, W. and Xu, R. 2004. The effects of total-body irradiation on the survival and skin wound healing of rats with combined radiation-wound injury. *J. Trauma.* 57(5), 1087–1093.
- Reisz, J.A., Bansal, N., Qian, J., Zhao, W. and Furdui, C.M. 2014. Effects of ionizing radiation on biological molecules--mechanisms of damage and

- emerging methods of detection. *Antioxid. Redox. Signal.* 21(2), 260–292.
- Riekkii, R., Parikka, M., Jukkola, A., Salo, T., Risteli, J. and Oikarinen, A. 2002. Increased expression of collagen types I and III in human skin as a consequence of radiotherapy. *Arch. Dermatol. Res.* 294(4), 178–184.
- Soref, C.M. and Fahl, W.E. 2015. A new strategy to prevent chemotherapy and radiotherapy-induced alopecia using topically applied vasoconstrictor. *Int. J. Cancer.* 136(1), 195–203.
- Sultan, S.M., Stern, C.S., Allen, R.J., Jr, Thanik, V.D., Chang, C.C., Nguyen, P.D., Canizares, O., Szpalski, C., Saadeh, P.B., Warren, S.M., Coleman, S.R. and Hazen, A. 2011. Human fat grafting alleviates radiation skin damage in a murine model. *Plast. Reconstr. Surg.* 128(2), 363–372.
- van Hezewijk, M., Creutzberg, C.L., Putter, H., Chin, A., Schneider, I., Hoogeveen, M., Willemze, R. and Marijnen, C.A. 2010. Efficacy of a hypofractionated schedule in electron beam radiotherapy for epithelial skin cancer: analysis of 434 cases. *Radiother. Oncol.* 95(2), 245–249.
- Wang, X.J., Lin, S., Kang, H.F., Dai, Z.J., Bai, M.H., Ma, X.L., Ma, X.B., Liu, M.J., Liu, X.X. and Wang, B.F. 2013. The effect of RHIZOMA COPTIDIS and COPTIS CHINENSIS aqueous extract on radiation-induced skin injury in a rat model. *BMC. Complement. Altern. Med.* 13, 105.
- Wang, Q., Zhou, Y., Wang, X. and Evers, B.M. 2006. Glycogen synthase kinase-3 is a negative regulator of extracellular signal-regulated kinase. *Oncogene* 25(1), 43–50.
- Ward, W.F., Molteni, A., Ts'ao, C. and Hinz, J.M. 1990. The effect of captopril on benign and malignant reactions in irradiated rat skin. *Br. J. Radiol.* 63(749), 349–354.
- Yoshimura, M., Itasaka, S., Harada, H. and Hiraoka, M. 2013. Microenvironment and radiation therapy. *Biomed. Res. Int.* 2013, 685308.
- Zhang, J.A., Yin, Z., Ma, L.W., Yin, Z.Q., Hu, Y.Y., Xu, Y., Wu, D., Permatasari, F., Luo, D. and Zhou, B.R. 2014. The protective effect of baicalin against UVB irradiation induced photoaging: an *in vitro* and *in vivo* study. *PLoS One* 9(6), e99703.